Design of Low-Cost Multimode Fiber Fed Indoor Wireless Networks Benito Sanz-Izquierdo, Anjali Das, Anthony Nkansah, Nathan J. Gomes, Ignacio J. Garcia, John C. Batchelor, and David Wake.

The link to this paper on IEEE Xplore® is
http://dx.doi.org/10.1109/TMTT.2006.877835

The DOI is: 10.1109/TMTT.2006.877835

Design of Low-Cost Multimode Fiber Fed Indoor Wireless Networks

Benito Sanz-Izquierdo, Anjali Das, Anthony Nkansah, Nathan J. Gomes, Ignacio J. Garcia, John C. Batchelor, and David Wake.

ABSTRACT

A low-cost option for transporting global system for mobile communication, Universal Mobile Telecommunication System and wideband local area network (WLAN) signals using multimode fiber (MMF) with 850-nm vertical-cavity surface-emitting lasers (VCSELs) is investigated through range predictions from a link budget analysis. These predictions are experimentally verified for WLAN signal transmission in an office environment, using a commercial access point and a 300-m (OM1/OM2) MMF link with low-cost 850-nm VCSEL transmitters. The analysis indicates that good performance and signal coverage is possible with optimum design of indoor fiber-fed wireless systems, even when using such inexpensive components.

Index Terms—Distributed antenna systems (DASs), multimode fiber (MMF), radio-over-fiber, vertical-cavity surface-emitting lasers (VCSELs), wireless local area networks (WLANs).

I. INTRODUCTION

RADIO-OVER-FIBER-BASED distributed antenna systems (DASs) can enable the deployment of picocellular access networks, providing high-quality mobile/wireless services for dense in-building user populations [1]. The use of multimode fiber (MMF) in such systems is attractive as it continues to be deployed in greater volumes than single-mode fiber, with typical installation lengths of up to 300 m [2]. Further, it has been shown that the MMF may be used for the transmission of RF carriers beyond the modal dispersion limited 3-dB bandwidth [3], [4]. For the DAS to be implemented with low incremental cost for the overall wireless network, inexpensive components such as vertical-cavity surface-emitting laser (VCSEL) transmitters can be used. Indeed, it has been shown that short-wavelength VCSELs can provide low distortion performance close to that of Fabry–Perot and distributed feedback (DFB) lasers for analog links [5]. For a DAS, the transmission of different radio signals over the same fiber-optic infrastructure would be of interest to neutral host providers. At shortwavelengths where component costs are less, a 300-m link comprising 850-nm multimode VCSEL and high-bandwidth MMF has been demonstrated with a spurious- free dynamic range (SFDR) of 94 dB $Hz^{2/3}$ in the frequency range of 1–8 GHz [6]. Good signal performance has also been reported for the transmission of emulated WLAN signals at 2.4 and 5 GHz over a VCSEL–MMF link [7]. Error-free transmission of GSM1800 and emulated Universal Mobile Telecommunication System (UMTS) signals using 850-nm VCSEL and 50/125- m MMF has also been shown in [8]. However, the experiments in [6]–[8] characterize only the optical link performance. Wireless path characterization is important as it has an impact on the link performance due to multipath signal fading. Moreover, bi-directional operation using real wireless signals over a VCSEL–MMF link has additional restrictions compared to emulated signal transmission.

In this paper, we analyze the link performance for a DAS fed by VCSEL–MMF-based optical links. A detailed link budget analysis is verified by experimental measurements on a wireless local area network (WLAN) demonstrator. The link budget analysis is then used to optimize remote antenna unit (RAU) design and predict maximum coverage ranges for WLANs,

GSM900, GSM1800, and UMTS.

II. SYSTEM LINK BUDGET

The basic DAS may be divided into four main parts, which are: 1) the central unit (CU); 2) the optical link; 3) the RAU; and 4) the mobile unit (MU), as shown in Fig. 1. The RF signal fed to the downlink (DL) path modulates the CU laser; the RF modulated optical signal is sent over the 300-m MMF link to the RAU. At the RAU, the incoming DL signal is detected by a photodiode (PD) and the retrieved RF signal is amplified and transmitted over the wireless path. For the uplink (UL), the received RF signal is first amplified and then fed to a laser in the RAU. The modulated optical signal is again sent over 300-m MMF and detected by a PD at the CU. For the RAU, a two-antenna design (using separate transmit and receive antennas), as shown in Fig. 2, is considered in this paper. Although a single antenna RAU may offer reduced size, for broadband operation, the greater isolation offered by using separate antennas enables the use of higher amplification levels and, hence, greater radio ranges. The effect of the isolation on the level of amplification possible will become apparent below. The link budget analysis that follows allows radio range predictions for the two-antenna RAU. The analysis can be divided into:

1) wireless path;
2) DL optical path; and
3) UL optical path calculations.

A. Wireless Path

The Keenan–Motley propagation model [9] is frequently used for calculating path loss (PL) in indoor environments. However, when the effects of transmission loss through walls and floors are ignored, the Keenan–Motley equation reduces to the openspace PL equation with a modified PL exponent *n* [10]

$$\mathrm{PL} = \left(\frac{4\pi f}{c}\right)^2 d^n. \tag{1}$$

Here, *f* is the frequency of the RF signal, is the velocity of light, and is the distance between the transmitter and receiver. The PL exponent *n* is a characteristic of the propagation environment and typically takes on values from 3 to 4 for indoor environments.

B. DL Optical Path

The input RF power ($P_{in,RF}$) to the CU laser needs to be such that distortion is avoided. This is especially important for systems using OFDM modulation (e.g., IEEE802.11g at 54 Mb/s) [11]. Once $P_{in,RF}$ has been set, the DL transmit power (P_t) is calculated as

$$P_t = \left(\frac{P_{\mathrm{in,RF}}}{L_{\mathrm{opt,dl}}}\right) G_{\mathrm{dl}} G_{\mathrm{au}} \tag{2}$$

where G_{dl} is the DL amplifier gain and G_{au} is the RAU antenna gain. $L_{opt,dl}$ is defined as the DL optical link insertion loss and is calculated as

$$L_{\mathrm{opt,dl}} = \frac{1}{\left\{ (\eta_{\mathrm{cu}} \alpha G_{\mathrm{fdl}} R_{\mathrm{pau}})^2 \frac{Z_{\mathrm{pau}}}{Z_{\mathrm{lcu}}} \right\}} \qquad (3)$$

where η_{cu} is the slope efficiency of the CU laser, G_{fdl} is the gain of the DL MMF (at any particular frequency), is the RAU PD impedance, and Z_{lcu} is the CU laser impedance, and the parameter α takes into account laser frequency response variations, which would not be modeled using the static slope efficiency.

Using P_t, the maximum tolerable propagation loss may be calculated as

$$L_{\mathrm{dl}} = \frac{(P_t G_{\mathrm{at}})}{S_{\mathrm{dl}}} \qquad (4)$$

where S_{dl} is the DL receiver sensitivity specified for each standard and G_{at} is the mobile terminal antenna gain. The above calculated loss can be matched against the propagation loss values calculated using (1) to find the maximum achievable range for the DL.

C. UL Optical Path

The UL radio-range calculations depend ultimately on the receiver equipment sensitivity at the CU, defined in terms of a minimum detectable signal (S_{uls}), the value of which is obtained from the standards (or may be specified by the equipment manufacturer). This leads to a minimum RF power required to drive the UL laser, and a minimum UL power at the receive antenna (S_{uls}). However, additional noise from the optical link increases the total UL noise floor, which, in turn, causes an increase in . The final value of the UL minimum detectable signal (S_{ul}) may then be written as

$$S_{\mathrm{ul}} = S_{\mathrm{uls}} + \left(\frac{C}{N}\right) N_{\mathrm{tot}} \qquad (5)$$

where *C/N* is the required carrier-to-noise ratio at the receiver specified in the relevant documents for each standard and N_{tot} is the total output UL noise power defined as

$$N_{\mathrm{tot}} = (\mathrm{NF}_{\mathrm{tot}}) k T g_{\mathrm{tot}} \qquad (6)$$

where *k* is Boltzmann's constant, *T* is the ambient room temperature (290 K), and g_{tot} and NF_{tot} are the cascaded gain and cascaded noise figure of the overall UL subsystem, respectively, using the standard cascade relationships [12]. For calculating NF_{tot} , the noise figure of the optical link needs to be determined as

$$\mathrm{NF}_{\mathrm{opt}} = \frac{(N_{\mathrm{opt}} L_{\mathrm{opt,ul}})}{kT} \quad (7)$$

where N_{opt} is the total noise power at the output of the optical link and $L_{opt,ul}$ is the UL optical insertion loss.
N_{opt} is defined as

$$N_{\mathrm{opt}} = N_{\mathrm{rin}} + N_{\mathrm{sh}} + N_{\mathrm{th}} \quad (8)$$

where N_{rin} is the RIN noise power, N_{sh} is the shot noise power, and N_{th} is the thermal noise power measured at the output of the CU PD. The other noise powers are calculated as

$$N_{\mathrm{sh}} = 2qZ_{\mathrm{pcu}} I_{\mathrm{ph}} \quad (9a)$$

$$N_{\mathrm{rin}} = (\mathrm{RIN}) {I_{\mathrm{ph}}}^2 Z_{\mathrm{pcu}} \quad (9b)$$

where q is the electronic charge, Z_{pcu} is the CU PD impedance, I_{ph} is the dc photocurrent, and RIN is the relative intensity noise of the laser. Both N_{th} and RIN demonstrate frequency dependence and were, therefore, experimentally determined for each of the standards.
As the UL and DL paths are similar, $L_{opt,ul}$ may be calculated in the same way as (6)

$$L_{\mathrm{opt,ul}} = \frac{1}{\left\{ (\eta_{\mathrm{au}} \alpha G_{\mathrm{ful}} R_{\mathrm{pcu}})^2 \frac{Z_{\mathrm{pcu}}}{Z_{\mathrm{lau}}} \right\}} \quad (10)$$

where η_{au} is the RAU laser slope efficiency, G_{ful} is the gain of the ULMMF (determined from the MMF response), R_{pcu} is the CU PD responsivity, and Z_{lau} is the RAU laser impedance.
Once N_{tot} is calculated and S_{ul} is determined, P_r is calculated as

$$P_r = \frac{(S_{\mathrm{ul}} L_{\mathrm{opt,ul}})}{(G_{\mathrm{au}} G_{up})} \quad (11)$$

where $L_{opt,ul}$ is the UL optical insertion loss and G_{up} is the UL amplifier gain.
The maximum tolerable UL propagation loss (L_{ul}) is then calculated as

$$L_{\mathrm{ul}} = \frac{P_{mt}}{P_r} \tag{12}$$

where P_{mt} is the mobile transmit power (and includes G_{at}) specified in the European Telecommunications Standards Institute (ETSI) documents for each standard. Using L_{ul}, the maximum achievable UL range may be determined by comparison with (1) in the same way as for the DL.

D. Additional Restrictions

Although the above equations represent the link budget for each direction of operation, further restrictions are posed in a real system.

1) Loop Gain: The RAU subsystem forms a loop with its DL and UL branches, as shown in Fig. 2, due to imperfect isolation between the two antennas and due to RF coupling between the RF drive to the UL VCSEL and DL PD circuit. This results in DL bleed and UL bleed signals being coupled to the UL and DL, respectively.

To avoid oscillation (with some margin), the maximum loop gain was set to be less than -10 dB. The loop-gain condition may be written as

$$\frac{(G_{up}G_{\mathrm{dl}})}{(\gamma_a \gamma_{\mathrm{pl}})} \leq 0.1 \tag{13}$$

where γ_a is the isolation between the two antennas and γ_{pl} is the isolation between the DL and UL paths at the VCSEL-PD end of the RAU.

With such a margin for the loop gain, it has been calculated that the signal coupled back into the DL causes little interference to the actual DL signal, and that the increase in the total signal level for the UL (the signal applied to the RAU laser) is not increased significantly, thus having little effect on the capping limit discussed below.

2) Capping: In order to obtain low distortion performance for the UL, a maximum is set for the amplified RF power fed to the RAU laser ($P_{r,max}$). This maximum must not be exceeded even when the MU is at a minimum distance (d_{min}) from the receive antenna. Thus,

$$P_{r,\max} = P_{mt}\left(\frac{G_{\mathrm{au}}G_{up}}{L_{ul,\min}}\right) \tag{14}$$

where $L_{ul,min}$ is the PL at d_{min}. It should be noted that the results presented in this paper are capping limited.

3) Transmitted Noise: Equations similar to (7)–(9) were also used to calculate transmitted DL noise power components. This power must be within acceptable limits as defined by IEEE or ETSI [13] standards. The above calculations were automated and carried out iteratively such

that the restrictions posed limits on the amplifier gains that could be used in the link budget/range calculations.

III. SYSTEM PARAMETERS

The component parameters used as inputs to the link budget for the range calculations were experimentally determined and are listed in Table I. The transmission of different standards was possible as the RAU contains no filters and uses multiband antennas [14]. The parameters of the standards evaluated are listed in Table II. These system parameters have been taken from or calculated using 3GPP standards for GSM900 [15], GSM1800 (DCS) [15], and UMTS [16]–[19] and the IEEE802.11b/g [20], [21] standard. The data rate assumed for IEEE 802.11g is 54 Mb/s and for IEEE 802.11b, 11 Mb/s, and 12.2 kb/s users are assumed for UMTS.

IV. SYSTEM DEMONSTRATOR

A system demonstrator for transmission of WLAN signals has been used to practically verify the link budget calculations. The calculations were carried out for both IEEE 802.11b and 802.11g for the achievement of a radio range (in both UL and DL) of 5 m, to cover a target room of size 6 m × 5 m, containing typical office furniture. The results are shown in Table III.

A. Experimental Setup

Fig. 3 shows the complete experimental setup of the WLAN system demonstrator. The CU and the RAU are placed in separate rooms and connected by 300-m MMF. The WLAN signal is generated using a commercial access point (AP) (*D-Link DWL-AP2000+*). ULM VCSELs operating at 850 nm are used as optical transmitters for both the DL and UL paths. An RF attenuator attenuates the WLAN signal before it is fed to the DL VCSEL to avoid distortion. Standard 50/125 m (OM1) and 62.5/125 μm (OM2) MMF, with lengths of 300 μm, are used for the DL and UL, respectively. The amplifier gains are adjusted to the values given in Table III through bias control.

For the measurements, the RAU was mounted on the ceiling towards one end of the room. The MU is a laptop with a wire-less card (D-Link AirPlusG DWL-G650) installed. TheMU had line-of-sight at all times with the RAU, although multipath effects were apparent.

TABLE I
INPUT PARAMETERS TO THE LINK BUDGET

Downlink:		
Component	Parameter	Measured/Used
VCSEL	Threshold current (I_{th})	1.5mA
	Bias current (I_b)	7mA
	Slope efficiency (η_{cu})	0.5W/A
	RIN[a] (RIN_{cu})	-128dB/Hz
	Impedance (Zl_{cu})	50 ohms
	Frequency factor (α)	-2.4dB
	Input RF Power ($P_{in,RF}$)	0.41mW (-3.9dBm)
PD	Responsivity (R_{pau})	0.42A/W
	Impedance (Z_{pau})	50 ohms
MMF 50/125μm	Gain (G_{fdl})	0.43 (-3.7dB)
Uplink:		
Component	Parameter	Measured/Used
VCSEL	Threshold current (I_{th})	1.5mA
	Bias current (I_b)	7mA
	Slope efficiency (η_{au})	0.38W/A
	RIN[b] (RIN_{au})	-144dB/Hz
	Impedance (Z_{lau})	50 ohms
	Frequency factor (α)	-2.4dB
	Max. input RF power ($P_{r,max}$)	0.41mW (-3.9dBm)
PD	Responsivity (R_{pcu})	0.44A/W
	Impedance (Z_{pcu})	50 ohms
MMF 62.5/125μm	Gain (G_{ful})	0.27 (-5.7dB)
Wireless Path:		
Component	Parameter	Measured/Used
Antenna (MU)	Gain (G_{at})	0dB
Antenna (RAU)	Gain (G_{au})	0dB
	Path loss exponent (n)[c]	3.2
Two antenna RAU:		
Component	Parameter	Measured/Used
	Antenna isolation (γ_a)	25dB
	Isolation at PD-VCSEL end (γ_{PL})	55dB
Central unit:		
Component	Parameter	Measured/Used
Circulator	Insertion loss (L_{cir})	0.5dB
Isolator	Insertion loss (L_{iso1})	0.5dB

[a, b] RIN values specified are measured at 2.4GHz. RIN values for the different systems have been listed in Appendix.

[c] n was empirically determined for the target office room by carrying out radiation measurements in the room.

TABLE II
SYSTEM PARAMETERS

System	Frequency (GHz)		S (dBm)		P_{mt} (dBm)	B (Mhz)	CNR (dB)
	DL	UL	DL	UL			
GSM 900	0.93	0.89	-102	-88	33	0.2	9
GSM 1800	1.8	1.71	-100	-95	30	0.2	9
UMTS (FDD)	2.11	1.92	-107	-107	27	3.84	15.1
UMTS (TDD)	2.01	2.01	-105	-95	24	3.84	15.1
802.11b	2.4	2.4	-82	-82	17	11	7
802.11g	2.4	2.4	-68	-68	17	11	24.8

TABLE III
CALCULATIONS FOR THE SYSTEM DEMONSTRATOR

System	Range (m)	Amplifier Gain (dB)		P_t (dBm)	DL Transmitted Noise Power (dBm)
		DL	UL		
802.11b	5	12.7	1.7	-19.6	-57.5
802.11g	5	26.7	12.1	-5.6	-43.5

B. Measurements and Results

The received signal strength at the MU was measured using commercial software (Wireless Network Ignition), which itself was checked against measurements with an electrical spectrum analyzer (Agilent E4407B) and known antenna. Fig. 4(a) and (b) shows the variation of signal strength with distance from the RAU for both IEEE 802.11b and IEEE 802.11g signals. As expected, the received signal strength is seen to generally decrease as the MU moves away from the RAU. The predicted signal strength from the link budget calculations is also plotted and, as can be seen, there is a close match between the two for both standards.

The link quality was tested by streaming a video signal over the link. It was possible to obtain high-quality signal reception throughout the room. In order to quantify the link performance, throughput measurements were carried out using Networx commercial software during the data transfer of a large file over the link. The average throughput against distance from the

RAU is plotted in Fig. 5 for both the 802.11b and 802.11g standards. Throughputs as high as 5.2 Mb/s for the IEEE 802.11b and 20 Mb/s for the IEEE 802.11g (at 54 Mb/s) were achieved closer to the RAU. These values are very close to the approximate maximum throughput values of 6 Mb/s for IEEE 802.11b and 22 Mb/s for IEEE 802.11g (at 54 Mb/s) reported in the literature [22]. From Fig. 5(a), it is seen that for IEEE 802.11b, the throughput values are relatively stable over the 5-m range. However, during the measurements for the IEEE 802.11g system, it was observed that on approaching the edge of the 5-m range, the data rate of the signal fluctuated between 54 and 36 Mb/s, due to fluctuations in signal strength (Fig. 4 shows average values). This leads to the decrease in the average throughput, even though the measured average signal strengths match predictions.

V. FUTURE SYSTEM OPTIMIZATION

The system demonstrator performance is limited by the available component specifications. We now compute the ranges for all systems presented in Section III when using the better available system components. For example, referring to Table I, it is assumed the lower RIN laser (with 0.38-W/A slope efficiency), the higher 0.44-A/W responsivity PD, and the 300-m OM1 MMF with gain -3.67 dB are available for both UL and DL. The remaining parameters are assumed the same as in Table I. The resulting radio range predictions for the different systems are then listed in Table IV. The range predictions are based only on the assumed system parameters of Table II.Within each system's bandwidth, the respective access protocol may be used to support multiple MUs depending on service requirements.

TABLE IV
POTENTIAL RANGE CALCULATIONS FOR DIFFERENT SYSTEMS

System	Range (m)	Amplifier Gain (dB)		P_t (dBm)	DL Transmitted Noise Power (dBm/Hz)	
		DL	UL		Required	Calculated
GSM 900	64	21.9	2.1	-12.4	-95	-152.03
GSM 1800	74	31.7	10.6	-2.6	-95	-142.23
UMTS (FDD)	23	9.6	10.7	-24.7	-90	-163.9
UMTS (TDD)	22	12.6	19.7	-21.8	-90	-134
IEEE 802.11b	40	43.6	26.4	9.2	-100.4	-114.54
IEEE 802.11g	12.4	38.4	26.7	4	-100.4	-119.5

The results in Table IV show that reasonable ranges can be obtained for all systems. In fact, it is unlikely that 30 m radius cells would be required for indoor coverage when the fiber link lengths are themselves typically no more than 300 m. System architectures can be envisaged where many RAUs provide the coverage for high-speed WLANs, whereas only subsets of these (simultaneously [23]) provide coverage for the less demanding systems.

The DL transmitted noise power was found to be in accordance with the spurious emission limit stated in each of the standards (the required noise power column in Table IV gives this value). However, the standards impose a much stricter limit on the spurious emission from a base station in another base-station's frequency band when co-locating different types of base stations or, in other words, where there is simultaneous transmission of different systems. In such a case, bandpass filters may be employed to further attenuate the noise power outside the wanted frequency band.

TABLE V
RIN VALUES FOR THE DIFFERENT STANDARDS

Frequencies (GHz)	RIN (dB/Hz)	
	DL	UL
0.9	-118.8	-137.5
1.8	-126.7	-138.6
2.0	-124.4	-136.5
2.4	-128	-144

VI. CONCLUSION

A link budget analysis has been developed for the bidirectional operation of a fiber-fed indoor wireless network. The analysis allows for the optimization of component values to obtain the best possible range, while taking into account restrictions such as crosstalk and noise emissions. A WLAN system demonstrator using low-cost components (VCSELs, OM1/OM2 MMF) has been used to verify the link budget predictions. The demonstrator also verifies the operation of the whole fiber-fed WLAN system, giving throughput values similar to those normally expected. Theoretical range predictions for different radio systems such as GSM900, GSM1800, UMTS [both frequency division duplex (FDD) and time division duplex (TDD)], as well as WLANs have been carried out for a system using the better measured component parameters. The results show that reasonable cell sizes may be achieved for all systems.

APPENDIX

RIN VALUES FOR THE DIFFERENT STANDARD FREQUENCIES

RIN values for the different standard frequencies for each of the DL and UL lasers were experimentally determined, and the values are listed in Table V.

ACKNOWLEDGMENT

The authors acknowledge many useful discussions with their colleagues in the virtual center Transmanche Telecom, and particularly J.-P. Vilcot, B. Sanz-Izquierdo, and J. Assaouré. The authors are also grateful to R. Davis, N. Simpson, T. Rockhill, and C. Birch for their assistance during the setup of the experiments.

REFERENCES

[1] D. Wake, "Trends and prospects for radio over fibre picocells," in *Int. Microw. Photon. Top. Meeting* , Awaji, Japan, Nov. 2002, pp. 21–24.

[2] A. Flatman, “In-premises optical fibre installed base analysis to 2007,” presented at the IEEE 802.310GBE Over FDDI Grade Fiber Study Group, Orlando, FL, Mar. 2004.
[3] D. Wake, S. Dupont, J.-P. Vilcot, and A. J. Seeds, “32-QAM radio transmission over multimode fibre beyond the fibre bandwidth,” in *Int. Microw. Photon. Top. Meeting*, Long Beach, CA, Jan. 2002, vol. supp., 4 pp.
[4] E. J. Tyler, M. Webster, R. V. Penty, and I. H. White, “Penalty free subcarrier modulated multimode fiber links for datacomm applications beyond the bandwidth limit,” *IEEE Photon. Technol. Lett.*, vol. 14, no. 1, pp. 110–112, Jan. 2002.
[5] R. V. Dalal, R. J. Ram, R. Helkey, H. Rousell, and K. D. Choquette, “Low distortion analog signal transmission using vertical cavity lasers,” *Electron. Lett.*, vol. 34, pp. 1590–1591, Aug. 1998.
[6] C. Carlsson, H. Martinsson, A. Larsson, and A. Alping, “High performance microwave link using a multimode VCSEL and high-bandwidth multimode fiber,” in *Int. Top. Microw. Photon. Meeting*, Long Beach, CA, Jan. 2002, pp. 81–84.
[7] M. Y. W. Chia, B. Luo, M. L. Yee, and E. J. Z. Hao, “Radio over multimode fibre transmission for wireless LAN using VCSELs,” *Electron. Lett.*, vol. 39, pp. 1143–1144, Jul. 2003.
[8] R. E. Schuh, A. Alping, and E. Sundberg, “Penalty-free GSM-1800 and WCDMA radio-over-fibre transmission using multimode fibre and 850 nm VCSEL,” *Electron. Lett.*, vol. 39, pp. 512–514, Mar. 2003.
[9] T. S. Rapapport and S. Sandhu, “Radio-wave propagation for emerging wireless personal-communication systems,” *IEEE Antennas Propag. Mag.*, vol. 36, pp. 14–23, Oct. 1994.
[10] *ASH Transceiver Designer’s Guide*. Dallas, TX: RF Monolithic Inc., 2004, p. 51.
[11] H. Sasai, T. Niiho, K. Tanaka, and K. Utsumi, “Radio over fiber transmission performance of OFDMsignal for dual-band wireless LAN systems,” in *Int. Microw. Photon. Topical Meeting*, Budapest, Hungary, Sep. 2003, pp. 139–142.
[12] T. S. Rappaport, *Wireless communications— Principles and practice*. Upper Saddle River, NJ: Prentice-Hall, 1996, pp. 565–568, Appendix B.
[13] *Radio Equipment and Systems (RES); Wideband Transmission Systems; Technical Characteristics and Test Conditions for Data Transmission Equipment Operating in the 2,4 GHz ISM Band and Using Spread Spectrum Modulation Techniques*, ETSI 300 328, Nov. 1996.
[14] *B. Sanz-Izquierdo, J. Batchelor, and R. Langley, “Broadband multifunction planar PIFA antenna,” in Loughborough Antennas Propag. Conf., Loughborough, U.K., Apr. 2005, pp. 209–212.*
[15] *3rd Generation Partnership Project; Technical Specification Group GSM/EDGE Radio Access Network; Radio Transmission and Reception, 3GPP TS 45.005, 2004-11, ver. 6.7.0.*
[16] *Universal Mobile Telecommunications System (UMTS); User Equipment (UE) Radio Transmission and Reception (FDD), 3GPP TS 25.101, 2003-03, ver. 6.7.0, rel. 6.*
[17] *Universal Mobile Telecommunications system (UMTS); User Equipment (UE) Radio Transmission and Reception (TDD), 3GPP TS 25.102, 2003-12, ver. 6.0.0, rel. 6.*
[18] *Universal Mobile Telecommunications system (UMTS); Base Station (BS) Radio Transmission and Reception (FDD), 3GPP TS 25.104, 2004-12, ver. 6.8.0, rel. 6.*
[19] *Universal Mobile Telecommunications system (UMTS); Base Station (BS) Radio Transmission and Reception (TDD), 3GPP TS 25.105, 2004-12, ver. 6.2.0, rel. 6.*
[20] *Supplement to IEEE Standard for Information Technology—Telecommunications and Information Exchange Between Systems—Local and Metropolitan Area Networks—Specific Requirements—Part 11: Wireless LAN Medium Access Control (MAC) and Physical Layer (PHY) Specifications: Higher-Speed Physical Layer Extension in the 2.4 GHz Band, IEEE Standard 802.11b-1999, 1999.*

[21] *Supplement to IEEE Standard for Information Technology—Telecommunications and Information Exchange Between Systems—Local and Metropolitan Area Networks—Specific Requirements Part 11: Wireless LAN Medium Access Control (MAC) and Physical Layer (PHY) Specifications Amendment 4: Further Higher Data Rate Extension in the 2.4 GHz Band, IEEE Standard 802.11g-2003, 2003.*
[22] *R. Seide, "Capacity, coverage, and deployment considerations for IEEE 802.11g, white paper," Cisco Syst., San Jose, CA, 2003.*
[23] A. Nkansah, A. Das, I. J. Garcia, C. Lethien, J.-P. Vilcot, N. J. Gomes, J. C. Batchelor, and D.Wake, "Simultaneous transmission of dual-band radio signals over a multimode fibre fed indoor wireless network," *IEEE Microw. Wireless Compon. Lett.*, submitted for publication.

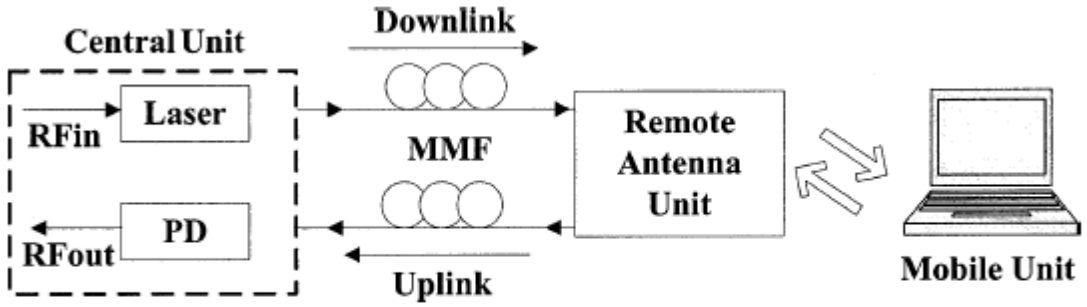

Fig. 1. Basic fiber-fed DAS.

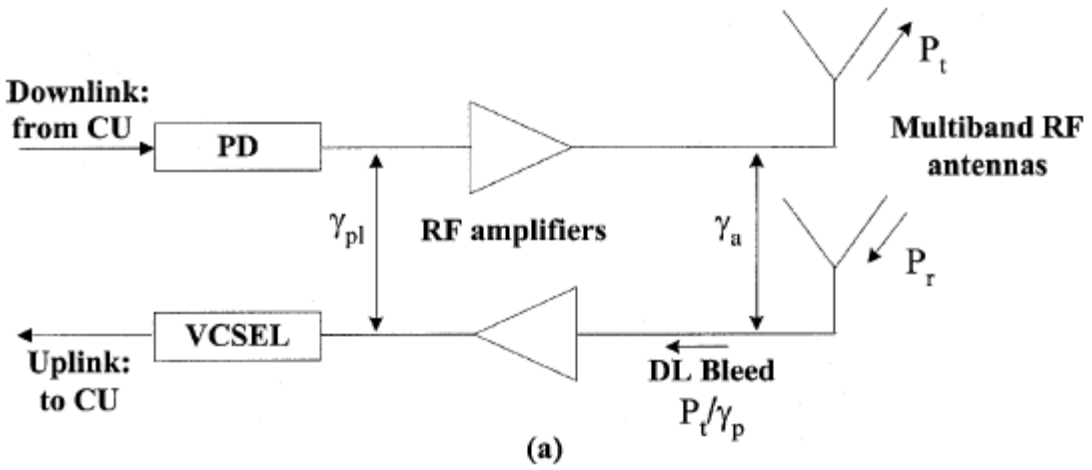

Fig. 2. Two-antenna RAU design.

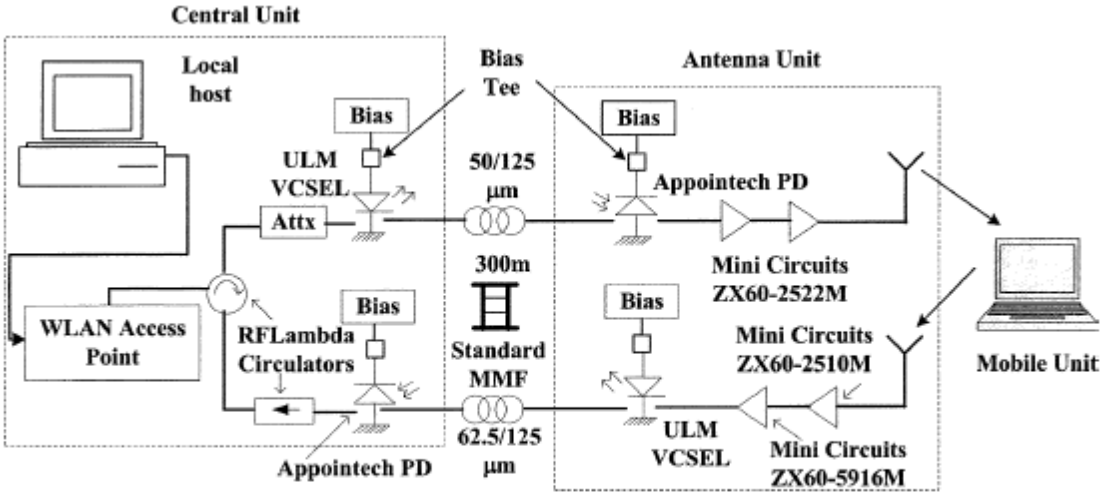

Fig. 3. Experimental setup of the system demonstrator.

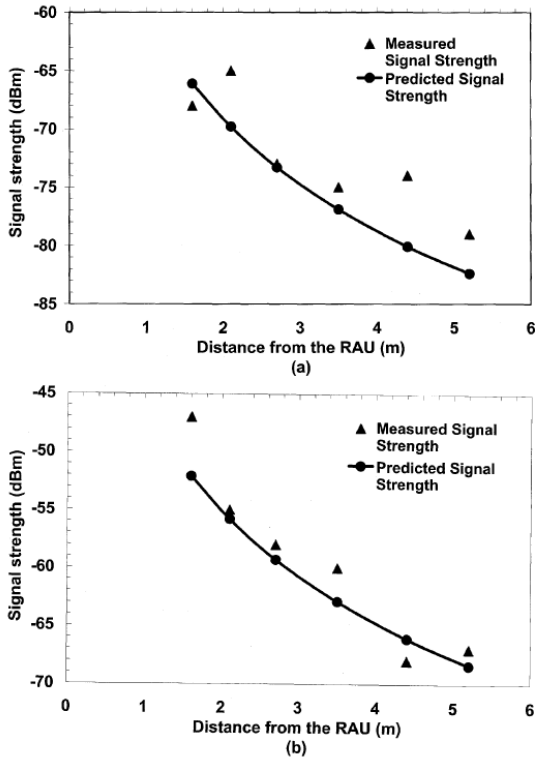

Fig. 4. Received signal strength for: (a) IEEE 802.11b and (b) IEEE 802.11g.

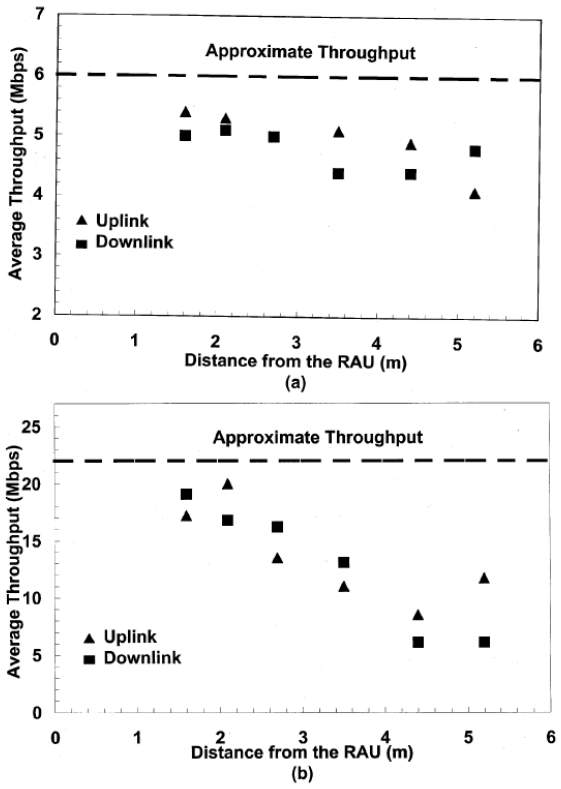

Fig. 5. Throughput measurement for: (a) IEEE 802.11b and (b) IEEE 802.11g.